

RESEARCH

Open Access



# Study the impact of transient state on the doubly fed induction generator for various wind speeds

Batoul Amen Alsati<sup>1\*</sup> , Ghassan Issa Ibrahim<sup>1</sup> and Rami Ramadan Moussa<sup>1</sup>

\*Correspondence:  
balsati@albaath-univ.edu.sy

<sup>1</sup> Department of Electrical Engineering, Faculty of Engineering, Al-Baath University, Homs, Syria

## Abstract

Recently, renewable resources such as wind, hydro, and tidal have experienced a rapid development. Electricity production, based on wind, has been concentrated on a large scale. Additionally, a doubly fed induction generator has been used in wind farms on a large scale. This machine is influenced by the multiple transient states that are happening in the grid. Many researchers studied the effect of voltage-dip on DFIG performance; none of them studied the effect of voltage-dip sharing with wind-speed changing for both sub- and hyper-synchronous modes. In this paper, DFIG behavior is investigated under a transient state which is represented by 3-phase voltage-dip, in both operation modes (sub-synchronous & hyper-synchronous) with various values of the wind speed. Based on MATLAB Simulink, the various DFIG parameters are extracted to determine the relation between voltage-dip, variable wind speed, and DFIG performance. Results show that the parameters that are affected were rotor-current, rotor-voltage, and DC-Link voltage, while stator-current and stator-flux are not affected. It is also shown that DC-Link voltage values are smaller in the hyper-synchronous mode compared with sub-synchronous one.

**Keywords:** Rotor-current, Wind speed, Voltage-dip, Transient state, Doubly fed induction generator (DFIG), DC-Link voltage

## Introduction

Recently, wind energy has been widely employed for its positive effect on the environment decreased cost and more advantages. Generally, wind-turbine generators are designed to be variable or fixed speed. Undoubtedly, doubly fed induction generator (DFIG) is one of the major technologies for wind-turbine WT manufacturers. It is suitable cost [1] and has the ability to provide a power to grid at constant frequency and voltage with variable rotor speed [2]. Despite the previous features, DFIG has some drawbacks such as absorption of reactive power and disability to control the voltage in existence of the rotor variable speed; thus, power converters should be used. The basic feature is to integrate power converters with DFIG that is the small fraction of the total power which is provided by the DFIG stator and which in turn connects to the power grid directly [3]. Size, overall costs, and power losses of power converters for DFIG are

smaller compared to full-size power converter. The rotor side of this machine could be operated at multiple rotationally speeds; by this way, the optimized ayro-dynamic efficiency could be achieved. Therefore, DFIG could operate in two modes: the first one is the sub-synchronous, and the other is the super-synchronous [4]. The voltage disturbances could be named as “voltage-dips.” This term illustrates the drop of the grid voltage due to fault occurrence in the power system [5]. WT based on DFIG is influenced by these disturbances at the contact point; this could also influence on the power converters and contactors of this system [6]. Voltage sag impacts on both DFIG and the power system, active power (P) is decreased, and the reactive power (Q) is increased. Moreover, the dc-bus voltage is increased to a considerable value, and the rotor-current has a considerable magnitude. Chen et al. [7] explained the total-harmonic distortion of the DFIG parameters under multiple kinds of voltage-dip with various magnitudes [8]. Voltage sag is basically associated with faults, and it may happen due to massive loads or during starting the large power machines [9]. When voltage-dip occurs, the stator is directly impacted [10]. Due to the electromagnetic connection between stator and rotor winding, voltage disturbance on the stator causes a considerable EMF in the rotor winding, which leads to create overcurrents in the rotor. These overcurrents have the ability to damage the semiconductor’s elements at RSC, and therefore, the DFIG is disconnected [11]. Majority of countries improved their codes related to WT connected with power grids, to keep reliability and quality in power grid. According to these codes, WTs should remain connected to the grid during voltage disturbance and after recovering its normal value [12]. Ref. [13] observed that overvoltage which is produced by voltage-dips may damage the DC-Link capacitor. Overcurrent is created in the rotor due to losing RSC control when voltage-dip is occurred [14]. According to [15], high magnitude of voltage-dip causes a high overvoltage on the DC-Link. Therefore, a current passes in the DC-Link due to power direction reversing. Stator-flux magnitude is shifted from normal magnitude to a novel steady-state magnitude [16]. Some researchers such as [17] concentrated on the dynamic performance of DFIG and the effects of excitation system based on RSC and GSC converters, by decreasing the transitive relationship of the transient cases. According to [18], PI controllers should be employed to regulate the RSC and GSC to control P&Q powers for both normal and transient operation conditions. Duggirala and Gundavarapu [19] investigated the instability that is resulted due to the voltage swells; stator-flux decay during the voltage swell is not occurred rapidly. Makhoba [20] investigated the basic challenges that are associated with voltage disturbances and determined the causes of these dips [21]. Presented the dynamic operation of DFIG under single-phase fault. Previous works are concentrated on the impact of voltage-dip on DFIG performance with a specified wind speed. Actually, wind system works with variable wind speed; thus, it is necessary to take into consideration the wind speed changes. It is found that previous studies concentrated on study DFIG performance under distribution for a fixed wind speed to facilitate the parameters’ observation; none of them has taken into consideration the variation of the wind speed. Therefore, there is a main question about as follows: How the variable wind speed could affect on DFIG performance under voltage-dip? And in this paper, we would define these effects to answer the study question.

Our work aims to investigate DFIG performance under voltage-dip for multiple wind speeds to determine the impact of these factors on DFIG performance as the following:

- 1- Investigate the impact of voltage-dip on (rotor-current, stator-current, stator-flux, rotor-voltage, DC-Link voltage) in sub-synchronous mode (7.5, 8, 8.5) wind speeds.
- 2- Investigate the impact of voltage-dip on (rotor-current, stator-current, stator-flux, rotor-voltage, DC-Link voltage) in hyper-synchronous mode (10, 10.5, 11, 11.5) wind speeds.

**Background**

A three-phase voltage grid is applied directly to the DFIG stator; this creates a magnetic field in the stator windings [1]. For DFIG rotor, the supply is achieved by varying voltage and frequency to reach various operating conditions such as torque and speed. To implement this, a 3-phase back-to-back converter should be used. Figure 1 represents the general structure of WT based on DFIG.

DFIG has the ability to operate in three various modes according to the slip sign. There are three various modes of operation [22]:

- Sub-synchronous:  $S > 0$
- Hyper-synchronous  $S < 0$
- Synchronous  $S = 0$

The operation with multi-speeds is implemented by managing the rotor circuit using an external device represented by electronic converters. Figure 1 presented the direct connection of the DFIG stator to the grid. However, the rotor is tied by power converters to the grid. By this way, the power is exchanged by these converters with the grid [23]. By controlling the RSC, the generator speed is regulated to implement the highest extraction of wind energy, thereby working in sub-synchronous and hyper-synchronous modes [24].

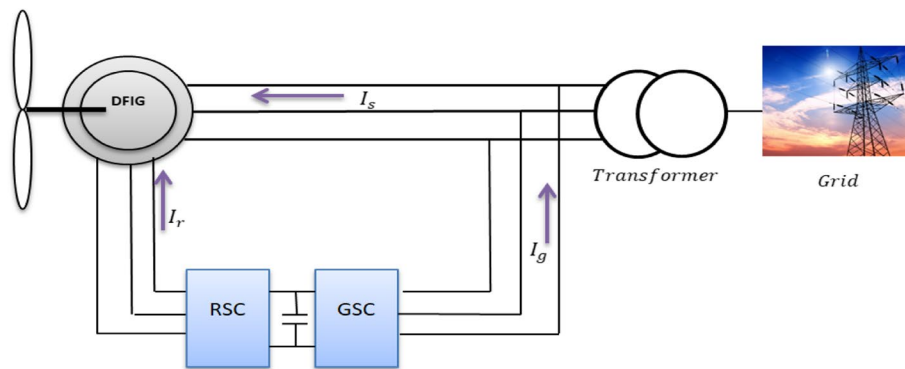


**Fig. 1** The basic structure of DFIG

**Methods**

**Modeling the system of wind energy based on DFIG**

Wind system based on the DFIG consists basically of wind turbine, back-to-back converters, and the doubly fed induction machine as a generator. These components are represented mathematically.

**Aerodynamic representation of the turbine**

This model evaluates mechanical torque for air flowing on the turbine, to compute the rotor output power. Wind velocity is defined by the wind average quantity which is caught on the area of the turbine’s rotating blade; the torque of turbine’s rotor is formulated as follows [25]:

$$T_m = \frac{1}{2} \rho \times C_t(\lambda) \pi V_\omega^2 R^3 (N.m) \tag{1}$$

where R: rotor’s radius of WT,  $\rho$ : air density,  $V_\omega$ : wind speed,  $C_p$ : coefficient of power (defined by the parameters of WT),  $\beta$ : turbine’s pitch –angle, and  $\lambda$ : tip – speed ratio.

$$\lambda = \frac{2\pi R n_r}{60 V_\omega} \tag{2}$$

There is a relation between  $C_p$  and the coefficient of torque  $C_t$ :

$$C_p(\lambda, \beta) = \lambda C_t(\lambda) \tag{3}$$

Mechanical energy of the wind farm could be formulated as follows:

$$P_m = \frac{1}{2} \rho \times C_p(\lambda, \beta) \pi R^2 V_\omega^3 \tag{4}$$

**DFIG representation mathematically**

Based on Park transformation, the 3-phase quantities of DFIG machine are transformed to dq reference frame as shown in the Fig. 2:

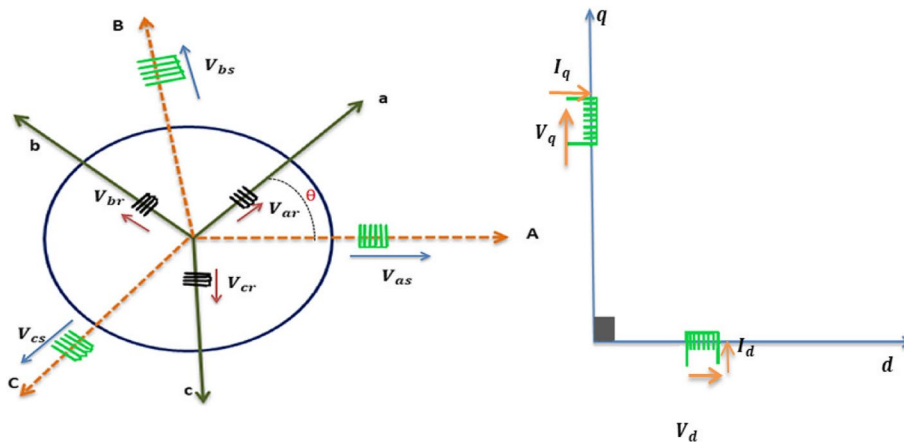


**Fig. 2** Park transformation (dq) for (DFIG)

According to [26, 27], the mathematical equations could be as follows:

$$V_{ds} = R_s i_{ds} + \frac{d\Psi_s}{dt} - \omega_s \Psi_{qs} \tag{5}$$

$$V_{qs} = R_s i_{qs} + \frac{d\Psi_s}{dt} + \omega_s \Psi_{ds} \tag{6}$$

$$V_{dr} = R_r i_{dr} - \omega_r \sigma L_r i_{qr} + \sigma L_r \frac{d}{dt} i_{dr} + \frac{L_m}{L_s} \frac{d}{dt} \Psi_{ds} \tag{7}$$

$$V_{qr} = R_r i_{qr} + \omega_r \sigma L_r i_{dr} + \sigma L_r \frac{d}{dt} i_{qr} + \omega_r \frac{d}{dt} \Psi_{ds} \tag{8}$$

$V_{ds}, V_{qs}, i_{ds}, \Psi_{ds}$ : Represent stator voltage, stator current, and stator-flux, respectively, according to  $d$ -axis,  $R_s$ : stator resistance

$V_{dr}, V_{qr}, i_{dr}, \Psi_{dr}$ , rotor-voltage, rotor current, and rotor flux, respectively, according to  $q$ -axis.

$R_r$ : Rotor resistance,  $\omega_r$ : rotor speed  $\sigma$  is the machine's leakage coefficient.

$L_r$  and  $L_s$  represent rotor inductance and stator inductance respectively.

The formula of torque is represented as follows [28]:

$$T_{em} = -\frac{3}{2} PL(\varphi_{dr} i_{qr} - \varphi_{qr} i_{dr}) \tag{9}$$

where P: poles' machine number and  $L_r$  rotor inductance.

**Rotor-side converter (RSC)**

The main function of the RSC is active and reactive power regulation independently. This is achieved by the vector-control application [25]. The control strategy includes two control loops for rotor current to get the reference voltages. The control scheme is built based on Eqs. 7 and 8 [29]. RSC injecting currents into the rotor circuit which adjust the rotor speed values according to the wind speed change [30].

**Symmetric dip for the voltage**

Voltage-dip is defined as a decline in the amplitude of voltage for several milliseconds. There are two types of voltage dip: symmetrical and non-symmetrical [31, 32].

**Simulink implementation and discussion**

This section investigates the performance of DFIG to observe the basic voltage-dip effects for both sub- and hyper-synchronous modes. The WT and DFIG are modeled in the MATLAB Simulink environment. Power system consists of a 2 MW DFIG, and WT, and RSC and GSC control schemes. Figure 3 presented the implemented model in MATLAB. DFIG works at variable wind speeds (7.5, 8, 8.5) m/s for the sub-synchronous mode and (10, 10.5, 11, 11.5) m/s for the hyper-synchronous mode. DC-Link voltage value is 1150 V under steady-state operation. The symmetric voltage-dip occurred at 3 s and stopped at 3.5 s (Fig. 3).

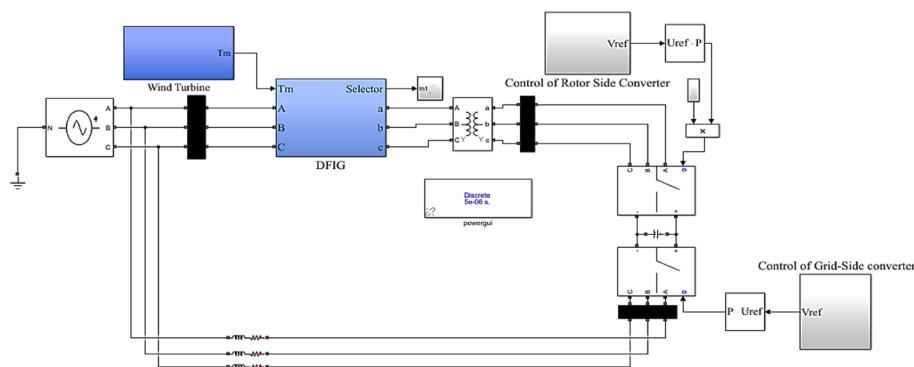


**Fig. 3** Block diagram of wind-system representation in MATLAB

Tables 1 and 2 show the parameters of the system that are used in this study.

### Results and discussion

The performance of DFIG is implemented under two operating modes (sub- & hyper-synchronous) under symmetric voltage-dip as the following:

#### Sub-synchronous

In this case, DFIG experiences a voltage-dip that is occurring at period time between 3 and 3.5 s and the wind speeds between 7.5, 8, and 8.5 m/s; both stator and rotor currents, DC-Link voltage stator-Flux, and rotor-voltage are measured for different wind speeds under symmetric voltage-dip. The measured parameters are summarized in Table 3.

**Table 1** The parameters of the simulated DFIG

Parameter	Value	Unit
$P_s$	$2 \times 10^6$	KW
$T_{em}$	12	KN.m
$V_s$	690	V
$n_{nominal}$	1500	r.p.m
Pole	2	--
$L_r$	$0.86 \times 10^{-3}$	mH
$L_s$	$0.86 \times 10^{-3}$	mH
$R_r$	0.025	ohm
$R_s$	0.027	ohm

**Table 2** The parameters of WT

Parameter	Value	Unit
Blade's radius	42	m
Wind speed	12.5	m/s
Max-min turbine	9-18	r, p, m
Ratio optimal-tip speed	7.2	--
$C_{pmax}$	0.44	--

**Table 3** The measured parameters of DFIG under voltage-dip and sub-synchronous mode

Wind speed (m/s)	$I_s$ (A)	$I_r$ (KA)	(IR)THD%	$V_r$ (V)	$V_{dc}$ (V)	$\varphi_s$ (WB)
7.5	10	4	75.33%	1183.7	1182	0.5
8	10	3.6	71.98%	1186.6	1181	0.5
8.5	11	3.4	62.09%	1181	1180	0.5

The symmetric voltage-dip is shown in Fig. 4. In this case, overcurrents in both stator and rotor are created; this impacts directly on the RSC and may lead to disconnect the wind system from the main grid, which reduce the reliability. Figure 5 shows the peak values of the rotor overcurrent for various wind-speed values. It is found that  $I_r$  got the highest peak at the wind-speed 7.5 m/s in the sub-synchronous mode, and it decreased by increasing the wind-speed value.

Despite that stator-current  $I_s$  is increased from its value before the dip to a higher value during the dip, it is not affected by the variance in wind speed. Additionally, stator-flux  $\varphi_s$  also is not affected by wind-speed variance; however, its value during the dip

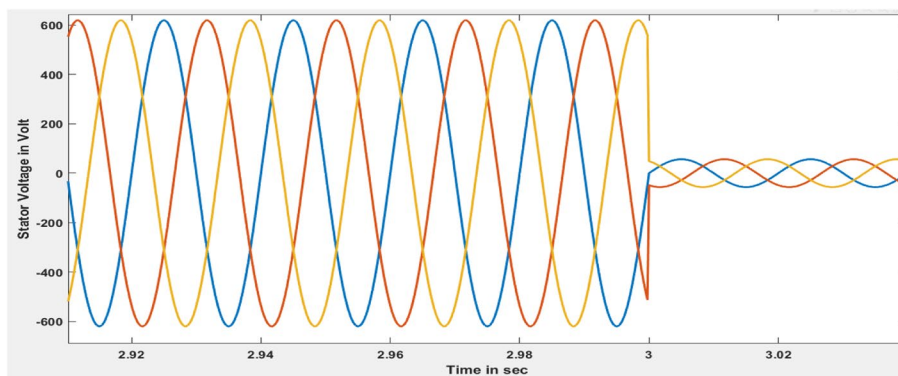


**Fig. 4** Voltage of the DFIG stator with dip at 3 s

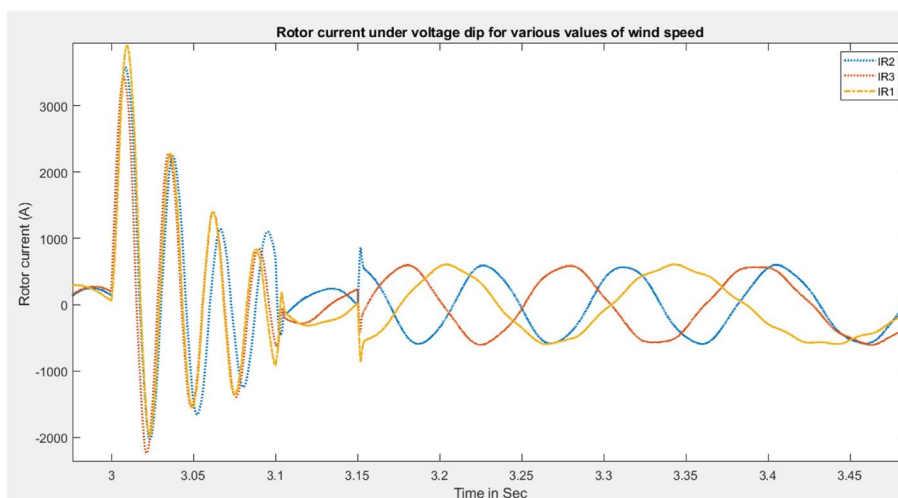


**Fig. 5** Rotor-current values under voltage-dip and sub-synchronous mode

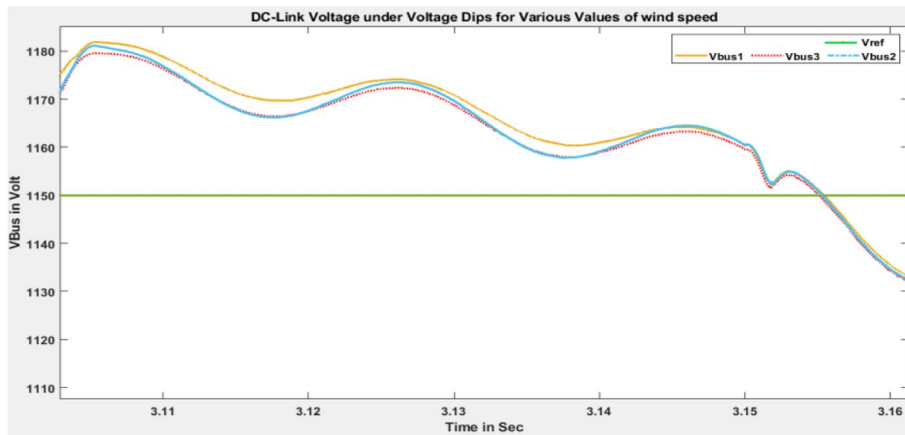


**Fig. 6** DC-Link voltage under voltage-dip and sub-synchronous mode

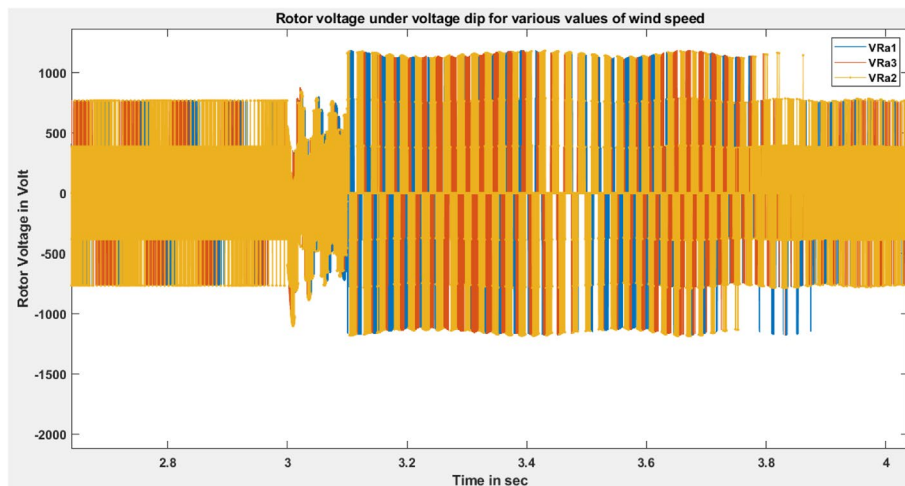


**Fig. 7** Rotor-voltage under voltage-dip and sub-synchronous mode

is smaller than its value before the dip. Stator-current and flux shape and behavior are agreed with [33, 34] for the same power 2 MW and at fixed wind speed. Moreover, over-voltages are appeared, and this also impacts on the DC-Link that might be deteriorated due to this overvoltages (Fig. 6). The DC-link voltage oscillates under and over the reference value (1150 V), and it was found that it is slightly affected by varying the wind speed. Based on fast Fourier transform (FFT), THD values are obtained for the measured rotor-current values. It could be seen from Table 1 that THD values are decreased when the rotor peaks are decreased. From Fig. 7. it could be observed that the effect of both, voltage-dip and the variable wind-speed, on the rotor-voltage. Generally, the disturbance in the voltage-grid impacts on rotor-voltage of DFIG and leads to create overcurrents with high magnitudes; however, after clearing the disturbance,  $V_r$  did not return to its value before the disturbance. It transforms to a new value that is higher than the normal value. This makes a challenge for the RSC operating during the voltage dip. Thereby, with variable wind-speed values, rotor-voltage is also changed (Figs. 7, 8 and 9).



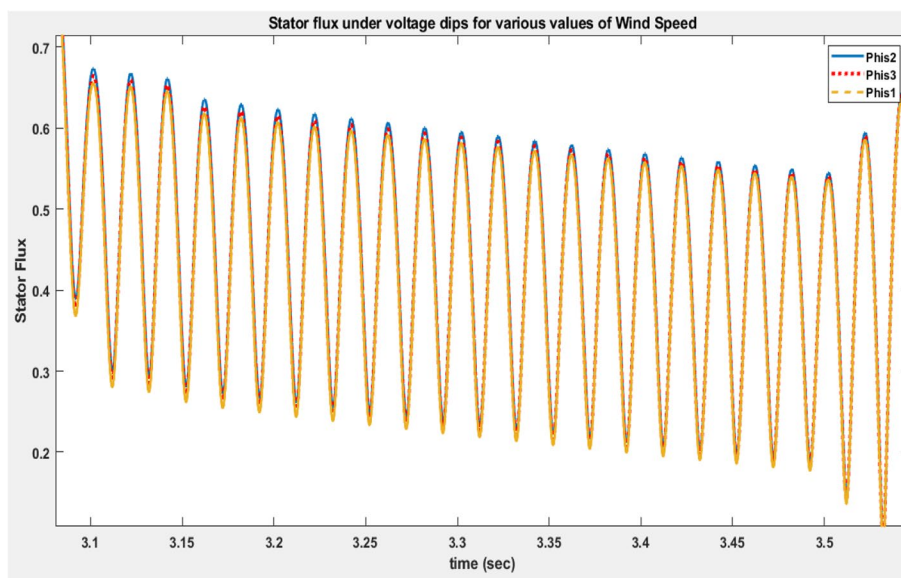


**Fig. 8** Stator-flux under voltage-dip and sub-synchronous mode

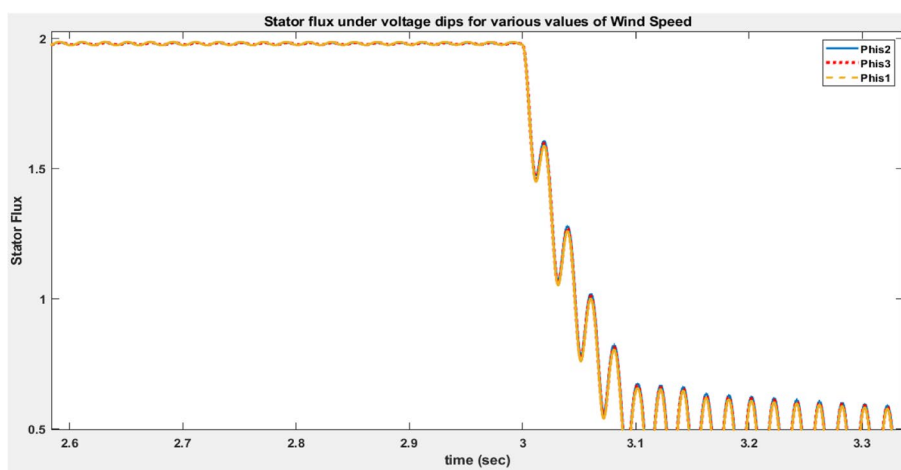


**Fig. 9** The impact of voltage-dip on  $\varphi_s$

**Hyper-synchronous**

DFIG performance is investigated in this section under voltage-dip which occurring at 3 to 3.5 s, with the hyper-synchronous speed between (10, 10.5, 11, 11.5) m/s. The measured DFIG parameters in this case are summarized in Table 4.

In this case,  $I_s, \varphi_s$  are affected only by the voltage-dip at 3 s, and results of these parameters are similar to the sub-synchronous mode’s ones. However, rotor current is decreased in this mode with the wind speed increasing to 10.5 m/s, and then it is increased for values that are higher than 11 m/s. In general, the voltage-dip impacts on the performance of DFIG for both sub-synchronous and super-synchronous operation modes. From the above results, it is obviously presented that the smaller values of rotor currents under voltage dips are achieved around 8 m/s for the wind speed (Fig. 10).

**Table 4** The measured parameters of DFIG under voltage-dip and sub-synchronous

Wind speed (m/s)	$I_s$ (A)	$I_r$ (KA)	(IR)THD%	$V_r$ (v)	$V_{dc}$ (V)	$\varphi_s$ (WB)
10	11.4	3.5	49.28%	1184	1178	0.5
10.5	11.5	3.77	40.86%	1178.4	1178	0.5
11	11.5	3.21	38.93%	1180	1178	0.5
11.5	11.2	4.13	29.18%	1179	1178	0.5

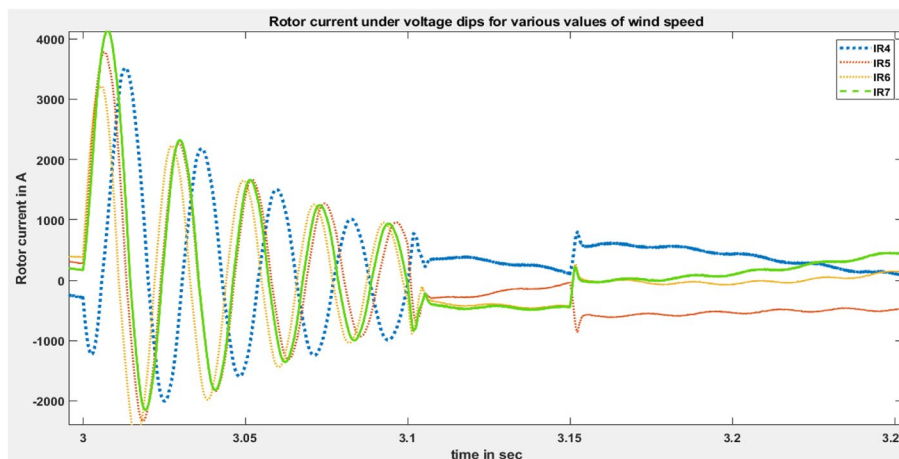


**Fig. 10** Rotor-current values under voltage-dip and hyper-synchronous mode

DC voltage is influenced by changing the operation mode from sub-synchronous to hyper-synchronous. DC-Link voltage values are smaller in the hyper-synchronous mode compared with sub-synchronous one in [12, 35]. For hyper-synchronous mode, the DC voltages have the same values for different wind speeds, and these values are higher than the reference value 1150 V. DC-Link voltage presents oscillations in this mode (Fig. 11). For the rotor-voltage  $V_r$ , its magnitude is also changed according to the variable wind speed. It is also transformed from the normal value before disturbance to a higher value after clearing the disturbance (Fig. 12).

**Conclusions**

DFIG provides a flexible behavior due to the ability to change the rotor speed according to variable wind speeds. However, DFIG has a set of challenges associated with its sensitivity to the disturbances that may occur in the grid. These disturbances impact on DFIG performance. In this study, the behavior of DFIG is investigated under symmetric voltage-dip for multiple values of wind speed for both modes (sub-synchronous & hyper-synchronous). From the results, it could be observed that the rotor current is reached to high values under voltage dip. In the sub-synchronous mode, rotor-current peak is increased during the voltage dip, with increasing the wind speed unlike the hyper-synchronous mode. These high currents impact on the RSC converter and increase the power losses; thus, it is necessary to improve the protection schemes to mitigate the high peaks of rotor currents. DC-Link is not affected by

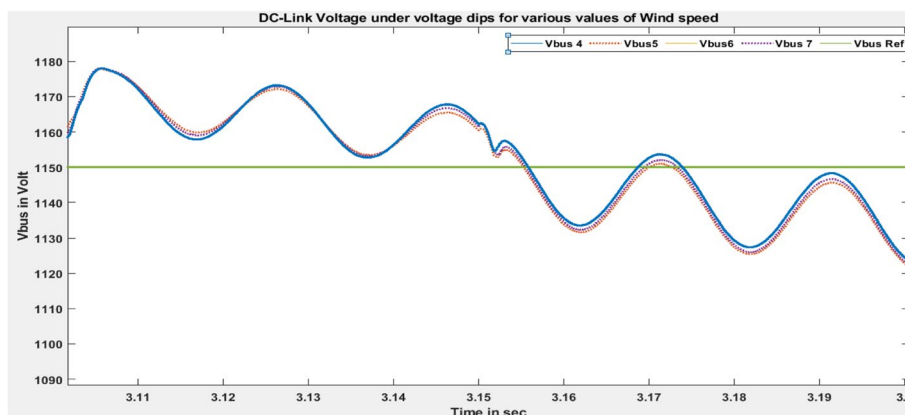


**Fig. 11** DC-Link voltage under voltage-dip & hyper-synchronous mode

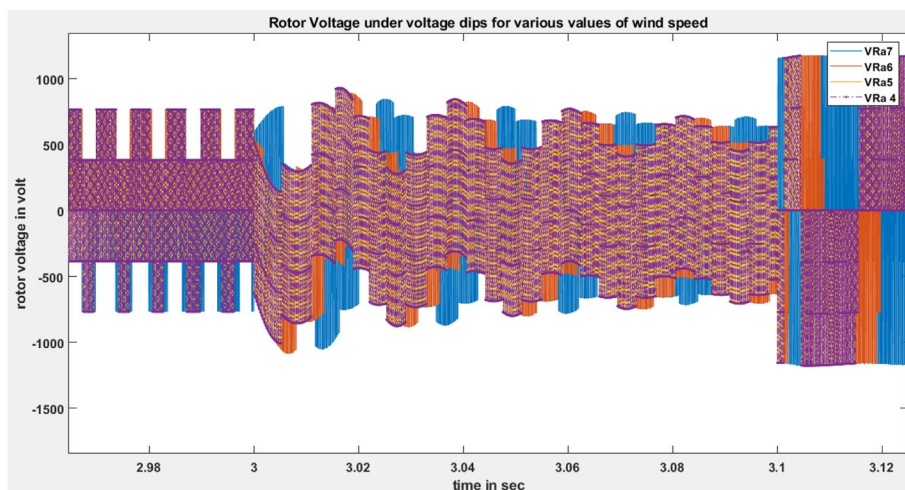


**Fig. 12** Rotor-voltage under voltage-dip and hyper-synchronous mode

the wind-speed variation, but its magnitude is increased during the voltage dip, and it presented oscillations. DC-Link should be protected from the overvoltage. Furthermore, overvoltages are created for both operation modes. Moreover, rotor-voltage is transformed from normal value before voltage-dip to a higher value after clearing the dip, this leads to some risks on RSC and DFIG performance, and stator-flux is affected only by the voltage-dip where it transformed from its normal value before the dip into higher value after clearing the dip. Overcurrents and overvoltages are considered as challenges for the power quality that is provided to the grid. Additionally, overcurrents cause power losses and damage the power converters. Generally, the voltage-dip effects lead to disconnect the wind system from the main grid. Therefore, DFIG should be equipped with powerful schemes such as crowbar, DC chopper, and FACTS device to improve its performance under voltage dip. At the end, in perspectives of this study, voltage-dip is considered a serious limitation for DFIG especially with variable speed that represents the actual operation of DFIG. It should develop powerful techniques having the ability to adopt with variable wind-speed to mitigate the voltage-dip sharing with changing wind-speed effects will be the aim of our future work.

**Abbreviations**

DFIG	Doubly fed induction-generator
WT	Wind turbine
$V_{ds}, V_{qs}, i_{ds}, \Psi_{ds}$	Stator (voltage, current, and flux) respectively according to $d$ -axis
$R_s$	Stator resistance
$V_{dr}, V_{qr}, i_{dr}, \Psi_{dr}$	Rotor (voltage, current, and flux) respectively according to $q$ -axis
$R_r$	Rotor resistance
$\sigma$	Machine's leakage coefficient
$T_{em}$	Electromagnetic torque
$P_s$	Power stator
RSC	Rotor-side converter
GSC	Grid-side converter

**Acknowledgements**

We would like to express our special thanks of gratitude to our Electrical Engineering Department, Al-Baath University, for facilitating and supporting this work.

**Authors' contributions**

BAA, conceptualization and methodology and writing. GI and RM, validation, verification, and supervision and writing review and editing. All authors have read and approved the manuscript.

**Funding**

The authors declare that they have not received any financial aid from any source in this study.

**Availability of data and materials**

The datasets generated and analyzed during the current study are available in the manuscript and attached files of tables and figures.

**Declarations****Competing interests**

The authors declare that they have no competing interests.

Received: 29 March 2023 Accepted: 8 June 2023

Published online: 26 June 2023

**References**

- Aljafari B, Pamela SJ, Vairavasundaram I, Singh RR (2022) Steady state modeling and performance analysis of a wind turbine-based doubly fed induction generator system with rotor control. *Energies* 15(9):3327. <https://doi.org/10.3390/en15093327>
- Chhipa AA, Chakrabarti P, Bolshev V, Chakrabarti T, Samarin G, Vasilyev AN, Kudryavtsev A (2022) Modeling and control strategy of wind energy conversion system with grid-connected doubly-fed induction generator. *Energies* 15(18):6694. <https://doi.org/10.3390/en15186694>
- Dannier A, Fedele E, Spina I, Brando G (2022) Doubly-fed induction generator (DFIG) in connected or weak grids for turbine-based wind energy conversion system. *Energies* 15(17):6402. <https://doi.org/10.3390/en15176402>
- Singh R (2017) Contrast the performance of doubly fed induction generator during symmetrical and non-symmetrical fault condition by varying wind speed, Master Thesis, School of Electronics and Electrical Engineering, Phagwara, Punjab
- Alshibani A, Hasanah, R, Suyono H (2018) Grid voltage dip impacts on the DFIG wind turbine and its main AC contactor performances. *Jurnal EEECCIS*; p. 54–60. doi: <https://doi.org/10.21776/jeeccis.v12i2.523>
- Rafiee Z, Rafiee M, Aghamohammadi M (2018) Effects of voltage sags on the doubly fed induction generator using PI controllers. Preprints. <https://doi.org/10.20944/preprints201806.0189.v1>
- Chen C, Bagheri A, Bollen M H, Bongiorno M (2019). The impact of voltage dips to low-voltage-ride-through capacity of doubly fed induction generator based wind turbine. In 2019 IEEE Milan PowerTech. IEEE; pp. 1–6. <https://doi.org/10.1109/PTC.2019.8810749>
- Kumar N, Chelliah TR, Srivastava SP (2016) Analysis of doubly-fed induction machine operating at motoring mode subjected to voltage sag. *Eng Sci Technol Int J* 19(3):1117–1131. <https://doi.org/10.1016/j.jestch.2016.01.015>
- Tang L, Han Y, Yang P, Wang C, Zalhaf AS (2022) A review of voltage sag control measures and equipment in power systems. *Energy Rep* 8:207–216. <https://doi.org/10.1016/j.egyr.2022.05.158>
- Qin B, Li H, Zhou X, Li J, Liu W (2020) Low-voltage ride-through techniques in DFIG-based wind turbines: a review. *Appl Sci* 10(6):2154. <https://doi.org/10.1109/IECON.2013.6700413>
- Soomro M, Memon ZA, Baloch MH, Mirjat NH, Kumar L, Tran QT, Zizzo G (2023) Performance improvement of grid-integrated doubly fed induction generator under asymmetrical and symmetrical faults. *Energies* 16(8):3350. <https://doi.org/10.3390/en16083350>
- Ansari AA, Dyanamina G (2022) Fault ride-through operation analysis of doubly fed induction generator-based wind energy conversion systems: a comparative review. *Energies* 15(21):8026. <https://doi.org/10.3390/en15218026>
- Zhou X, Tang Y, Shi J (2017) Enhancing LVRT capability of DFIG-based wind turbine systems with SMES series in the rotor side. *Int J Rotating Mach* 2017:1–8. <https://doi.org/10.1155/2017/4635452>

14. Ouyang J, Zheng D, Xiong X, Xiao C, Yu R (2016) Short-circuit current of doubly fed induction generator under partial and asymmetrical voltage drop. *Renew Energy* 88:1–11. <https://doi.org/10.1016/j.renene.2015.10.062>
15. Cheikh R, Belmili H, Menacer A, Drid S, Chrifi-Alaoui L (2019) Dynamic behavior analysis under a grid fault scenario of a 2 MW double fed induction generator-based wind turbine: comparative study of the reference frame orientation approach. *Int J Syst Assur Eng Manag* 10:632–643
16. Alsmadi YM, Xu L, Blaabjerg F, Ortega AJP, Abdelaziz AY, Wang A, Albatineh Z (2018) Detailed investigation and performance improvement of the dynamic behavior of grid-connected DFIG-based wind turbines under LVRT conditions. *IEEE Trans Ind Appl* 54(5):4795–4812. <https://doi.org/10.1109/TIA.2018.2835401>
17. Ouyang J, Xiong X (2014) Dynamic behavior of the excitation circuit of a doubly-fed induction generator under a symmetrical voltage drop. *Renew Energy* 71:629–638. <https://doi.org/10.1016/j.renene.2014.06.029>
18. Rafiee Z, Rafiee M, Aghamohammadi MR (2020) The voltage dip and doubly fed induction generator with considering uncertainty conditions. *Bull Electr Eng Inform* 9(1):30–38. <https://doi.org/10.11591/eei.v9i1.1669>
19. Duggirala VN, Gundavarapu V (2015) Dynamic stability improvement of grid connected DFIG using enhanced field oriented control technique for high voltage ride through. *J Renew Energy*. <https://doi.org/10.1155/2015/490178>
20. Makhoba K G (2020) Consideration of the effects of symmetrical and asymmetrical voltage dips in the control and operation of a grid-connected doubly-fed induction generator, (Doctoral dissertation) <https://researchspace.ukzn.ac.za/>
21. Wu YK, Shu WH, Liao JY, Wu WC (2019) Dynamic behavior of the doubly fed induction generator during three-phase and single-phase voltage dips IEEE 2nd International Conference on Knowledge Innovation and Invention (ICKII). *IEEE*; p. 149–152 | doi: <https://doi.org/10.1109/TEC.2006.878241>
22. Thomas T, Asok P (2020) Event analysis and real-time validation of doubly fed induction generator-based wind energy system with grid reactive power exchange under sub-synchronous and super-synchronous modes. *Eng Rep* 2(12):e12282. <https://doi.org/10.1002/eng2.12282>
23. Mwaniki J, Lin H, Dai Z (2017) A condensed introduction to the doubly fed induction generator wind energy conversion systems. *J Eng*. doi: <https://doi.org/10.1155/2017/2918281>
24. Herizi A (2020) Amelioration des performances de la commande non lineaire robuste d'un moteur asynchrone a double alimentation "mada" (doctoral dissertation, université m'sila). <http://dspace.univ-msila.dz:8080/>
25. Qi L, Jiahui W, Haiyun W, Hua Z, Jian Y (2023) Effect of DFIG control parameters on small signal stability in power systems. *Sci Rep* 13(1):2476
26. Mahalakshmi R, Viknesh J, Thampatty K S (2016) Mathematical modelling of grid connected doubly fed induction generator based wind farm. In 2016 IEEE International Conference on Power Electronics, Drives and Energy Systems (PEDES). *IEEE*; pp. 1–6. <https://doi.org/10.1109/PEDES.2016.7914301>
27. Ma Y, Zhu D, Zou X, Kang Y, Guerrero JM (2022) Transient characteristics and quantitative analysis of electromotive force for DFIG-based wind turbines during grid faults. *Chin J Electr Eng* 8(2):3–12. <https://doi.org/10.23919/CJEE.2022.000010>
28. Gupta R, Dyanamina G (2019) MATLAB simulation of DTC-SVM of doubly fed induction generator for wind energy system. In 2019 Innovations in Power and Advanced Computing Technologies (i-PACT). Vol. 1. *IEEE*; p. 1–6. <https://doi.org/10.1109/i-PACT44901.2019.8959990>
29. Singh R (2017) Contrast the performance of doubly fed induction generator during symmetrical and non-symmetrical fault condition by varying wind speed, master thesis, School of Electronics and Electrical Engineering Lovely Professional University. <http://dspace.lpu.in:8080/>
30. Ananth DVN, Kumar GN (2016) Fault ride-through enhancement using an enhanced field oriented control technique for converters of grid connected DFIG and STATCOM for different types of faults. *ISA Trans* 62:2–18. <https://doi.org/10.1016/j.isatra.2015.02.014>
31. Makhoba K G (2020). Consideration of the effects of symmetrical and asymmetrical voltage dips in the control and operation of a grid-connected doubly-fed induction generator (doctoral dissertation) <https://ukzn-dspace.ukzn.ac.za/>
32. Chung PD (2019) Voltage enhancement on DFIG based wind farm terminal during grid faults. *Eng Technol Appl Sci Res* 9(5):4783–4788. <https://doi.org/10.48084/etasr.3117>
33. Abdi Y (2022) Modeling, control, and analysis of doubly fed induction generator based on wind turbine system. Master thesis.
34. Ibrahim AA, Solomin EV (2018) Impacts of voltage dips in doubly fed induction motor for wind turbine generation systems. *Вестник Южно-Уральского государственного университета Серия: Энергетика* 18(4):41–51
35. Smina T, Beevi A, Ramalyer S (2020) Control of wind driven doubly fed induction generator under unbalanced grid voltage conditions. *Int J Appl Eng Res* 15:695–699

## Publisher's Note

Springer Nature remains neutral with regard to jurisdictional claims in published maps and institutional affiliations.